International Journal of Scientific Research in Mathematical and Statistical Sciences
Vol.**11**, Issue.**1**, pp.**61-68**, February **2024**
E-ISSN: 2348-4519
Available online at: www.isroset.org

Research Article

Mathematical Modelling of Magnetohydrodynamic Blood Flow through Slippery Small Arteries with Gold Nanoparticles for Breast Cancer Therapy

Adamu Garba Tahiru[1], Isah Abdullahi[2*], Idris Babaji Muhammad[3] Mahmood Abdulhameed[4], Mukhtar Abubakar Maiwada[5]

[1,3,5]Dept. of Mathematical Sciences, Bauchi State University, Gadau, Bauchi, Nigeria
[2]Dept. of Mathematical Sciences, Abubakar Tafawa Balewa University, Bauchi, Nigeria
[4]Dept. of Electrical &Electronics Engineering, Abubakar Tafawa Balewa University, Bauchi, Nigeria

**Corresponding Author: isahabdullahi7474@gmail.com, Tel: +2347039747474*

Received: 29/Dec/2023; **Accepted**: 24/Jan/2024; **Published**: 29/Feb/2024

Abstract— The research paper titled "Mathematical Modelling of Magnetohydrodynamic Blood Flow through Slippery Small Arteries with Gold Nanoparticles for Breast Cancer Therapy" introduces a novel methodology for breast cancer treatment. This approach integrates gold nanoparticles (AuNPs) into a mathematical model that accounts for magnetohydrodynamic (MHD) blood flow in small arteries. The primary objective is to enhance the precision and targeting of interventions in breast cancer therapy, aiming to minimize systemic side effects while maximizing therapeutic efficacy. The investigation explores the potential of AuNPs in targeted drug delivery, leveraging their distinctive physicochemical attributes and selective accumulation in Breast cancer tissues. Furthermore, the study incorporates MHD principles into the framework, emphasizing the impact of magnetic fields on blood flow dynamics and its implications for drug transport and distribution. Notably, the research underscores the significance of slip conditions in small arteries, which play a crucial role in influencing blood flow dynamics and are integral for accurately capturing the nuances of nanoparticle interactions. The study meticulously details the research methodology, encompassing problem formulation and the use of visual representations grounded in real-world scenarios related to the physical aspects of the system. The study's findings contribute to the existing knowledge base by presenting a comprehensive mathematical model that encapsulates the interplay of MHD blood flow, slip conditions, and gold nanoparticles within the specific context of breast cancer therapeutics. The research holds promise for optimizing drug delivery strategies in breast cancer treatments, providing valuable insights into the potential of this innovative approach to address the complexities associated with breast cancer and elevate the precision of drug delivery.

Keywords— Breast Cancer, Slippery Small Arteries, Gold Nanoparticles

1. Introduction

Breast cancer is a common and potentially fatal illness among women worldwide. Traditional treatment approaches, such as surgery, chemotherapy, and radiotherapy, have demonstrated efficacy. However, emerging research explores innovative strategies to enhance therapeutic outcomes and minimize side effects. One promising avenue involves the use of gold nanoparticles in conjunction with magnetohydrodynamic (MHD) blood flow through small arteries. This combination holds potential for targeted drug delivery and localized treatment of breast cancer. Breast cancer remains a significant health concern globally, with increasing incidence rates. Current treatment modalities, while effective, often result in systemic side effects. Chemotherapy, for example, can cause damage to healthy tissues along with cancerous cells. Thus, there is a growing interest in developing more precise and targeted approaches for breast cancer treatment. Due to its complexity and high incidence, breast cancer poses a serious threat to world health and is associated with high rates of morbidity and death.. Although conventional treatments have proven effective, their drawback lies in the manifestation of systemic side effects attributed to the non-specific distribution of therapeutic agents. Recognizing the imperative need for more precise and targeted interventions, this research embarks on an exploration of an innovative approach. It seeks to integrate gold nanoparticles (AuNPs) into breast cancer treatments through a sophisticated mathematical modeling framework that accounts for the magnetohydrodynamic (MHD) blood flow through slip small arteries. Breast cancer's complexity arises from its

diverse subtypes, variable clinical presentations, and the intricate interplay of genetic and environmental factors. Consequently, the conventional treatment landscape, predominantly featuring surgery, chemotherapy, and radiation, grapples with the challenge of achieving a delicate balance between eradicating cancer cells and minimizing harm to healthy tissues. The systemic side effects associated with non-targeted drug distribution, such as nausea, fatigue, and immunosuppression, underscore the pressing need for more refined therapeutic strategies [1,2]. Gold Nanoparticles (AuNPs) have emerged as promising entities in the realm of cancer therapy. Their unique physicochemical properties, including biocompatibility and the ability to be finely tuned for surface modifications, make them ideal candidates for drug delivery systems [3]. Moreover, their capacity to accumulate selectively in tumor the enhanced permeability and retention (EPR) effect is a phenomenon observed in tissues., presents an opportunity to mitigate off-target effects while concentrating therapeutic payloads at the tumor site [4]. Leveraging these attributes, the integration of AuNPs into breast cancer treatment holds potential for achieving a more targeted and efficient delivery of therapeutic agents.

To enhance the precision of drug delivery in breast cancer, this research incorporates the principles of magnetohydrodynamics (MHD) into the framework. MHD introduces a magnetic field into the dynamics of blood flow, influencing its behavior in ways that have implications for drug transport and distribution [5]. Understanding these influences is crucial for optimizing the delivery of therapeutic agents to cancerous tissues, as blood flow dynamics play a pivotal role in determining the transport pathways and kinetics of drug particles [6]. In small arteries, the concept of slip conditions becomes particularly significant. Slip conditions at the vessel walls impact the dynamics of blood flow, influencing factors such as velocity distribution and shear stress. Incorporating slip conditions into the mathematical model is essential for accurately capturing the intricacies of blood flow in small arteries, as this contributes to a more realistic representation of how Nanoparticles interact with.

The overarching objective of this research is to develop a comprehensive mathematical model that integrates the dynamics of MHD blood flow through slip small arteries with the presence of gold nanoparticles. By doing so, the study aims to provide insights into the optimization of drug delivery strategies for breast cancer treatments, with the ultimate goal of minimizing systemic side effects while maximizing the therapeutic impact.

2. Related Work

A significant body of research has delved into the mathematical modeling of various aspects of cancer therapeutics, ranging from drug pharmacokinetics to the understanding of tumor microenvironments. Notable studies, such as those by [1, 2], have underscored the importance of mathematical models in optimizing drug delivery strategies and predicting treatment outcomes. While these studies provide a foundational understanding of mathematical modeling in cancer research, the specific integration of magnetohydrodynamics (MHD) and slip conditions in small arteries with gold nanoparticles in breast cancer treatments is an area that demands further exploration. Several studies have investigated the use of gold nanoparticles (AuNPs) as carriers for anticancer drugs. The work of [3, 4], highlights the biocompatibility and tunability of AuNPs for targeted drug delivery. These investigations provide important new information about the therapeutic potential of AuNPs. But integrating these nanoparticles into an all-encompassing mathematical model that takes into account the particular dynamics of blood flow in narrow arteries is a novel strategy that deserves additional consideration. Studies by[5,6] have looked into the application of magnetohydrodynamics (MHD) principles in the setting of blood flow. These studies explore the effects of magnetic fields on blood flow dynamics, offering a theoretical framework for comprehending the ways in which MHD may affect the circulation's ability to deliver drugs. address. Studies like those of [7, 8, 21] have contributed to our understanding of slip situations in tiny arteries. These works explore the influence of slip conditions on blood flow patterns and provide valuable data for mathematical modeling. However, the incorporation of slip conditions into a comprehensive model alongside MHD and gold nanoparticles specifically tailored for breast cancer treatments is an innovative direction that this research aims to contribute to the existing body of knowledge. The related work reveals a foundation of knowledge in mathematical modeling, MHD, slip conditions, and gold nanoparticles individually within the context of cancer research. However, the integration of these elements for breast cancer treatments is an area where gaps persist. The proposed research seeks to leverage the existing knowledge while advancing the field by providing a comprehensive model that encapsulates the interplay of MHD blood flow, slip conditions, and gold nanoparticles in the specific context of breast cancer therapeutics.

3. Methodology

The purpose of this part is to provide a comprehensive analysis of the research methods applied in this study. The next step will be the formulation of problems using visual aids that are based on actual events related to the problem's physical characteristics. Here, the governing equations for momentum and energy are derived in cylindrical coordinates using the Navier-Stokes equation. These linear equations and partial differential equations (PDEs) sets represent the derived governing equations. The first stage is a depersonalization procedure in which the corresponding values in the governing equations and related conditions are substituted with dimensionless variables and the thermophysical properties of the nanofluid. The main aim of this approach is to achieve a dimensionless representation of the governing equation and associated conditions by eliminating inherent units. Through depersonalization, the study establishes dimensionless parameters like the Darcy number, magnetic parameter, Grashof number, and Prandtl number, which are essential for in-depth analysis and graphical representation. The subsequent section provides a

concise evaluation of recent technology, applications, or products. The research focuses on examining the incompressibility of human blood, incorporating gold nanoparticles (AuNPs) circulating through small arteries. The investigation explores the flow characteristics of a Casson fluid containing AuNPs within a cylindrical region defined by a radius denoted as r0. The z-axis represents the direction of Casson fluid motion, while the r-axis is perpendicular to the z-axis. Blood motion is a result of pulsatile flow induced by the heart's beating action and convection flow within the cylinder. A uniformly applied magnetic field, B0, operates along the r-axis, disregarding any induced magnetic and viscous dissipation. The study also looks into the impact of a porous medium representing fatty plaque or blood clots, and it considers slippage between blood flow and solid arteries. The physical representation of the issue is illustrated in Fig. 1, using r and t exclusively as constituents of blood velocity and temperature.

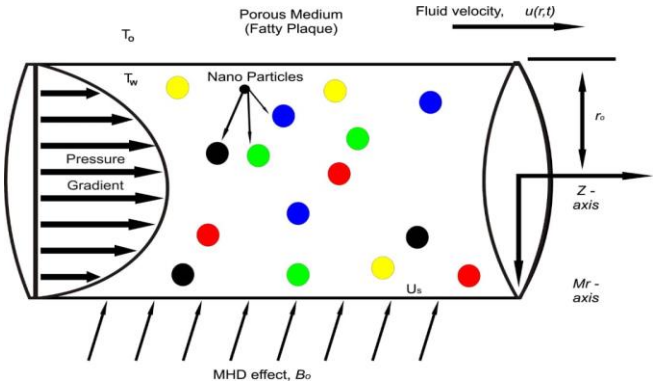

Figure 1; Schematic Diagram of blood flow in Arteries

The equation that dictates the connection between shear stress and strain rate in an incompressible flow of a Casson fluid is formulated as follows [9,10]:

$$\tau_{ij} = \begin{cases} 2\left(\mu_B + \dfrac{\tau_y}{\sqrt{2\pi}}\right)\ell_{ij}; \pi > \pi_c \\ 2\left(\mu_B + \dfrac{\tau_y}{\sqrt{2\pi_c}}\right)\ell_{ij}; \pi > \pi_c \end{cases} \quad (1)$$

The parameters in this context are defined as follows: $\pi = \ell_{ij}\ell_{ij}$ and ℓ_{ij} represents the the (i,j)-th constituent of the deformation rate, μ_B representing plastic dynamic viscosity, while τ_y signifies fluid yield stress, and π results from multiplying the deformation rate by itself. The critical value of this product, based on the non-Newtonian model, is denoted as π_c. The primary emphasis is on the Casson fluid model rather than the Papanastasiou-Casson regularization model, with the former being a more recent approach. The validation of current findings is supported by extensive research on the Casson fluid model over the past few decades [11]. The Casson fluid model is recognized for its simplicity compared to the Papanastasiou-Casson regularization model, leading many researchers to choose numerical investigations of the latter due to its complexity. Given the analytical approach in this study, the Casson fluid model is considered imperative. The governing equations for the problem, in line with Boussinesq's approximation, the Tiwari and Das nanofluid model, and the mentioned assumptions, are formulated as presented in references [12,13,21].

$$\left.\begin{aligned} &\rho_{nf}\frac{\partial \dot{u}_f(r,t)}{\partial \dot{t}} = -\frac{\partial \dot{p}}{\partial \dot{z}} + \mu_{nf}\left(1+\frac{1}{\beta}\right)\left(\frac{\partial^2 \dot{u}_f(r,t)}{\partial \dot{r}^2} + \frac{1}{\dot{r}}\frac{\partial \dot{u}(r,t)}{\partial \dot{r}}\right) - \delta_{nf}B_0^{\,2}\dot{u}_f(r,t) + \\ &\mathrm{KN}\quad (u_p - u_f) - \frac{\mu_{nf}}{k_p}\dot{u}_f + g(\beta\rho_{nf})(\mathrm{T}-\mathrm{T}_\infty) \end{aligned}\right\} \quad (2)$$

$$m\frac{\partial \dot{u}_p}{\partial \dot{t}} = \mathrm{K}_s(\dot{u}_f - \dot{u}_p) \quad (3)$$

$$\rho c_p\frac{\partial \dot{T}}{\partial \dot{t}} = \mathrm{K}_{nf}\left(\frac{\partial^2 \mathrm{T}}{\partial \dot{r}^2} + \frac{1}{\dot{r}}\frac{\partial \mathrm{T}}{\partial \dot{r}}\right) \quad (4)$$

In the context of the study, various parameters are defined: $\dot{u}$ represents the velocity component along the z-axis, $\dot{t}$ represents the time parameter, $\partial\dot{p}/\partial\dot{z}$ signifies a pulsatile pressure gradient, $\beta = \mu_B\sqrt{2\pi_c}/\tau_y$ denotes the non-Newtonian Casson parameter, B_0 represents the applied magnetic field strength, k_p is the permeability constant, g g is the gravitational acceleration, T represents the fluid temperature, and T_∞ represents the ambient temperature. Additionally, the thermophysical properties related to Casson nanofluids are detailed in [14], with the nanofluid's viscosity being roughly equivalent to that of the base fluid containing spherical nanoparticles, as emphasized by Brinkman [15]. At the initial time (t = 0), both the fluid and the cylinder are at rest. As time progresses (t > 0), the fluid starts moving with a slip velocity at the boundary. Simultaneously, the cylinder's temperature rises from to the boundary temperature and then remains constant. The initial and boundary conditions for the problem are provided in references [16,17,21] therein.

$$\left.\begin{aligned} &\dot{u}_f(r,o) = 0, \quad \mathrm{T}(r,0) = \mathrm{T}_\infty, \quad \dot{u}_p(r,o) = 0, \quad &&: r \in [0, r_0] \\ &\dot{u}_f(\dot{r}_0,t) = \dot{u}_s, \quad T(\dot{r}_0,\dot{t}) = T_w, \quad u_p(\dot{r}_0,\dot{t}) = u_s &&; t > 0 \end{aligned}\right\} \quad (5)$$

where $\dot{u}_s$, is the slip velocity condition. The relevant dimensionless variables are stated as [18–10]:

$$t = \frac{\dot{t}r}{r_0^{\,2}}, r = \frac{\dot{r}}{r_0}, u_f = \frac{\dot{u}_f}{u_0}, u_p = \frac{\dot{u}p}{u_0}, u_s = \frac{\dot{u}_s}{u_0}$$
$$, z = \frac{\dot{z}}{r_0}, p = \frac{\dot{p}}{\mu u_0}, \theta = \frac{\mathrm{T}-\mathrm{T}_\infty}{\mathrm{T}_w - \mathrm{T}_\infty} \quad (6)$$

The governing equations (2)-(4) along with conditions (5) are transformed into their dimensionless forms by utilizing the appropriate dimensionless variables, resulting in the following expressions.

$$\left.\begin{aligned}\frac{\partial u_f}{\partial t} = -b_5\frac{\partial \rho}{\partial z} + b_6\beta_1\left(\frac{\partial u_f}{\partial r^2}+\frac{1}{r}\frac{\partial u_f}{\partial r}\right)+\\ \mathrm{P}_c\left(u_p-u_f\right)-b_8\mathrm{M}u_f+b_9 Gr\theta(r,t)-\frac{b_6}{Da}u_f\end{aligned}\right\} \quad (7)$$

$$P_m\frac{\partial u_f}{\partial u_t} = u_f - u_p \quad (8)$$

$$\frac{\partial\theta(r,t)}{\partial t} = \frac{b_3}{\rho_r}\left(\frac{\partial^2\theta(r,t)}{\partial r^2}+\frac{1}{r}\frac{\partial\theta(r,t)}{\partial r}\right) \quad (9)$$

And the conditions:

$$\begin{aligned} &u_f(r,0)=0, \quad u_p(r,0)=0,\\ &\theta(r,0)=0 \quad ;r\in[0,1]\\ &u_f(1,t)=u_s, \quad u_\rho(1,t)=u_s,\\ &\theta(1,t)=1 \quad ;t>0\end{aligned} \quad (10)$$

Where;

$$\mathrm{M}=\frac{\delta_f r_0^2\mathrm{B}_0^2}{\mu_f}, Gr=\frac{g(\mathrm{B_T})f(\mathrm{T}_w-\mathrm{T}_\infty)r_0^2}{v_f u_0},$$

$$P_r=\frac{v_f(\rho c_p)}{\mathrm{K}_f}, P_m=\frac{\mathrm{M}v_f}{r_0^2\mathrm{K}_s}, P_c=\frac{\mathrm{KN}r_0^2}{\mu},$$

$$\beta_1=\frac{1}{\beta_0}, \beta_0=1+\frac{1}{\beta}$$

Are Magnetic field parameter, Grashof mass number, Prandtl number, Particle mass number, Particle Concentration Parameter and Casson fluid parameter respectively.

Moreover, $-\frac{\partial\rho}{\partial z}=\mathrm{A}_0+\mathrm{A}_1\cos(wt)$ represents the pulsatile pressure gradient, simulating the pumping motion of the heart [18]. where A0 and A1 correspond to the pulsatile amplitude, while ω denotes the pulsatile frequency. The dimensionless momentum governing equation can be expressed by rewriting this information:

$$\left.\begin{aligned}\frac{\partial u_f}{\partial t} = b_5\left(\mathrm{A}_0+\mathrm{A}_1\cos(\omega t)\right)+\\ b_6\beta_1\left(\frac{\partial^2 u_f}{\partial r^2}+\frac{1}{r}\frac{\partial u_f}{\partial r}\right)\\ +\rho_c\left(u_p-u_f\right)-\frac{b_6}{Da}u_f\\ -b_8\mathrm{M}u_f+b_9 Gr\theta\end{aligned}\right\} \quad (11)$$

4. Problem Solution

To evaluate blood flow within a slipping cylinder containing AuNPs, a comprehensive approach is required, combining Laplace and finite Hankel transforms. The finite Hankel transform is particularly advantageous for cylindrical domains, while the Laplace transform is useful for handling initial-boundary values and transient issues. The reduction of partial differential equations (PDEs) leads to ordinary differential equations (ODEs). By applying inverse transformations for both Laplace and finite Hankel, analytical results can be obtained.

Initially, the Laplace transform technique is applied to the dimensionless form of the energy governing equation (Eq. 9) and the corresponding dimensionless conditions (Eq. 10), resulting in:

$$s\bar{\theta}(r,s)=\frac{b_3}{\rho_r}\left[\frac{d^2\bar{\theta}(r,s)}{dr^2}+\frac{1}{r}\frac{d\bar{\theta}(r,s)}{dr}\right] \quad (12)$$

$$\bar{\theta}(1,s)=\frac{1}{s} \quad (13)$$

The Laplace transform of the function $\theta(r,t)$, denoted as $\bar{\theta}(r,s)$, is represented by, with the transformation variable being s. Subsequently, Eq. (12) undergoes transformation through the application of the zero-order finite Hankel transform, in conjunction with the condition (13), resulting in:

$$\bar{\theta}_H(r,s)=\frac{J_1(r_n)}{r_n}\left[\frac{1}{sP_r+b_3 r_n^2}\right] \quad (14)$$

Where $\bar{\theta}(r_n,s)=\int_0^1 r\bar{\theta}(r_n,s)J_0(rr_n)dr$ is the finite Hankel transform of the function $\theta(r,s)$and r_n with n = 0,1… are the positive roots of the equation $J_0(x)=0$, where J_0 is the Bessel function of the first kind and zero-order, and J_1 is the Bessel function of the first kind and first-order. Then, the result of simplifying Eq. (14) is:

$$\bar{\theta}_H(r,s)=\frac{J_1(r_n)}{r_n}\left[\frac{1}{s}-\frac{1}{s+\frac{b_3 r_n^2}{P_r}}\right] \quad (15)$$

In the next step, Eq. (15) undergoes the inverse Laplace transforms, yielding:

$$\bar{\theta}_H(r,t)=\frac{J_1(r_n)}{r_n}\left[1-\exp\left(\frac{-b_3 r_n^2 t}{P_r}\right)\right] \quad (16)$$

Ultimately, the analytical solution for the temperature profiles (Eq. 16) is derived by applying the inverse finite Hankel transform, resulting in:

$$\theta(r,t)=1-2\sum_{n=1}^{\infty}\frac{J_0(rr_n)}{r_nJ_1(r_n)}\frac{J_1(r_n)}{r_n}\exp\left[\frac{b_3r_n^2t}{P_r}\right] \quad (17)$$

The dimensionless Nanoparticles concentration and momentum equations (8) and (11). Both the equations and the corresponding conditions (equation 8) are solved using the Laplace transform, leading to the following outcome:

$$\bar{u}_p(r,s)=\frac{\bar{u}_f(r,s)}{sP_m+1} \quad (18)$$

$$\left.\begin{aligned} &s\bar{u}_f(r,s)=b_5\left(\frac{\mathrm{A}_0}{s}+\frac{\mathrm{A}_1 s}{s^2+\omega^2}\right)+\\ &b_6\beta_1\left(\frac{d^2\bar{u}_f(r,s)}{dr^2}+\frac{1}{r^2}\frac{d\bar{u}_f(r,s)}{dr}\right)-\\ &\frac{b_6}{Da}\bar{u}_f(r,s)-b_8\mathrm{M}\bar{u}_f(r,s)+\\ &P_c\left(\bar{u}_p(r,s)-\bar{u}_f(r,s)\right)+b_9Gr\bar{\theta}(r,s)\end{aligned}\right\} \quad (19)$$

$$\bar{u}(1,s)=\frac{u_s}{s} \quad (20)$$

Then Laplace's partial differential equations (18)–(19) with the corresponding condition in (20) are transformed into an ordinary differential equation (ODE) using the finite Hankel transform of zero-order, which is represented as follows:

$$\left.\begin{aligned} &s\bar{u}_{Hf}(r_n,s)=b_5\frac{J_1(r_n)}{r_n}\left(\frac{\mathrm{A}_0}{s}+\frac{\mathrm{A}_1 s}{s^2+\omega^2}\right)+\\ &b_6\beta_1\left[\frac{r_nJ_1(r,n)}{s}u_s-r_n^2\bar{u}_{Hf}(r_n,s)\right]\\ &-\frac{b_6}{Da}\bar{u}_{Hf}(r_n,s)-b_8\mathrm{M}\bar{u}_{Hf}(r_n,s)+\\ &P_c\left(\bar{u}_{Hp}(r_n,s)-\bar{u}_{Hf}(r_n,s)\right)\\ &+b_9Gr\theta_H(r_n,s)\end{aligned}\right\} \quad (21)$$

$$\bar{u}_{Hp}(r_n,s)=\frac{\bar{u}_{Hf}(r_n,s)}{sP_m+1} \quad (22)$$

Where $\bar{u}_H(r_n,s)=\int_0^1 r\bar{u}(r_n,s)J_0(rr_n)dr$ is the finite Hankel transform of the function $u(r,s)$ and r_n with n = 0,1… are the positive roots of the equation $J_0(x)=0$, where J_0 is the Bessel function of the first kind and zero-order, and J_1 is the Bessel function of the first kind and first-order.

On substituting (Eq,22) into (Eq,21) we the general momentum equation as;

$$\bar{u}_{Hf}(r,s)=\left[\begin{aligned} &\frac{b_5J_1(r,n)}{r_n}\left[\frac{\mathrm{A}_0}{s}+\mathrm{A}_1 s\big/ s^2+\omega^2\right]\\ &+\frac{b_6\beta_1J_1(r_n)}{s}u_s+\\ &b_9Gr\bar{\theta}_H(r,s)\end{aligned}\right]\frac{1}{s+b_{11}(n)} \quad (23)$$

Similarly, the Nanoparticles concentration equation is obtained by integrating equation (23) and (22) as:

$$\bar{u}_{Hp}(r_n,s)=\frac{1}{sP_m+1}\left[\begin{aligned} &\frac{b_5J_1(r,n)}{r_n}\left[\frac{\mathrm{A}_0}{s}+\frac{\mathrm{A}_1 s}{s^2+\omega^2}\right]+\\ &\frac{b_6\beta_1J_1(r_n)}{s}u_s\\ &+b_9Gr\bar{\theta}_H(r,s)\end{aligned}\right]\frac{1}{s+b_{11}(n)} \quad (24)$$

The inverse Laplace form of equation (23) and (24) with the aid of Gerby-Stefan's Algorithm and the results were simulated graphically with the aid of MATCARD software.

5. Results and Discussion

Pulsatile flow in a Casson nanofluid under the combined effects of slip, convective heat transfer, magnetohydrodynamics, and porosity is the subject of the present study. Both the Laplace transform and the finite Hankel transform are applied to this difficult situation. With respect to a number of parameters, such as the Casson parameter (β), magnetic parameter (M), Grashof number (Gr), Prandtl number (Pr), slip velocity parameter (us), particle mass parameter (Pm), particle concentration parameter (Pc), and the time parameter (t), the velocity, nanoparticle concentration, and temperature profiles are graphically represented. Refer to [19,20,21].

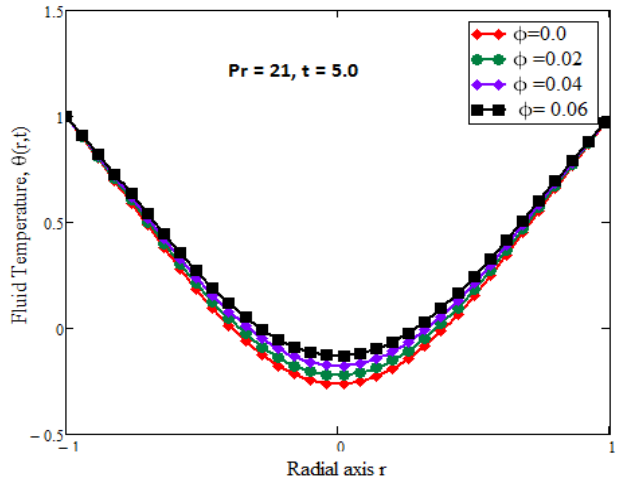

Fig.2; Nanoparticles volume fraction parameters influence temperature profiles

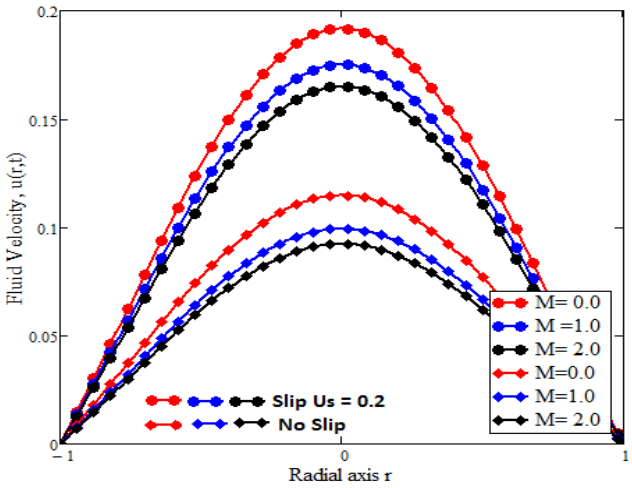

Fig.5;Magnetic parameter influence on fluid velocity profile at t = 5

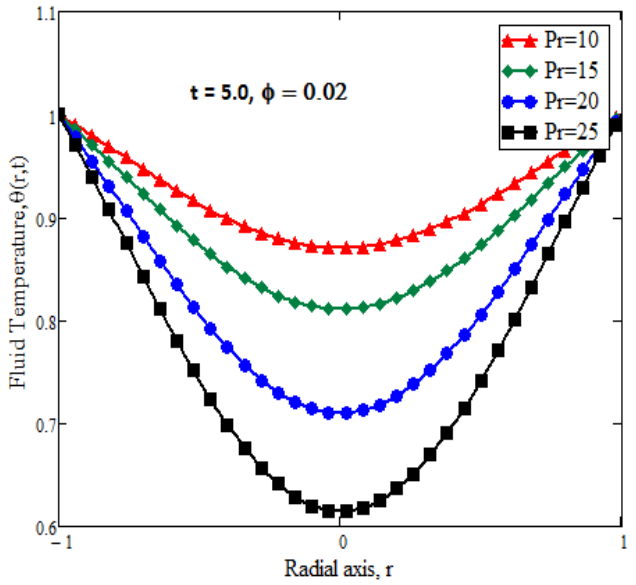

Fig.3; Prandtl number influence on temperature profiles

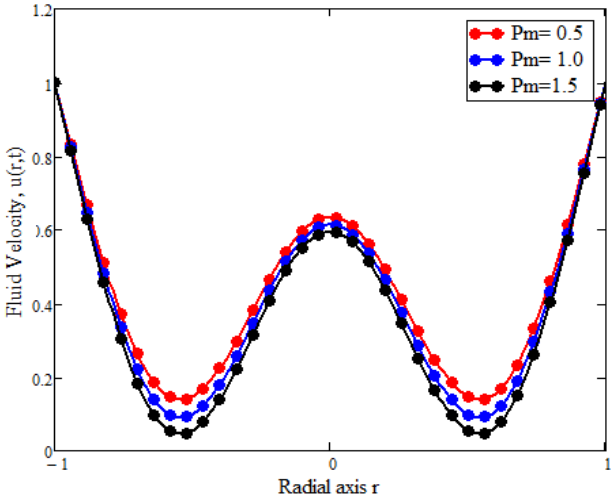

Fig.6; Particle mass parameter influence on fluid velocity profile at t = 5

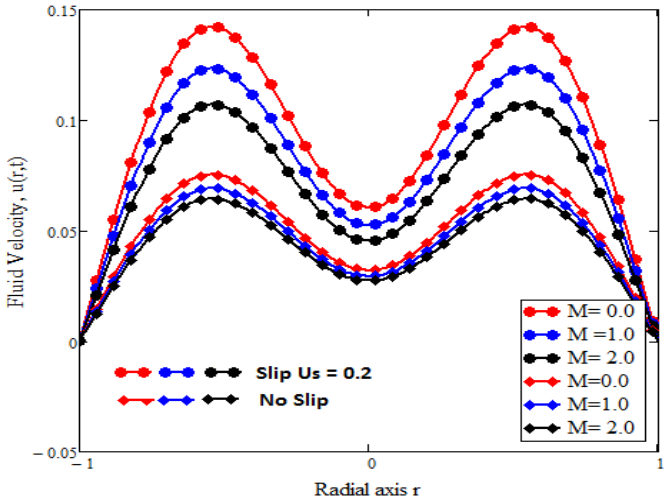

Fig.4; Magnetic parameter influence on fluid velocity profile at t = 0.6

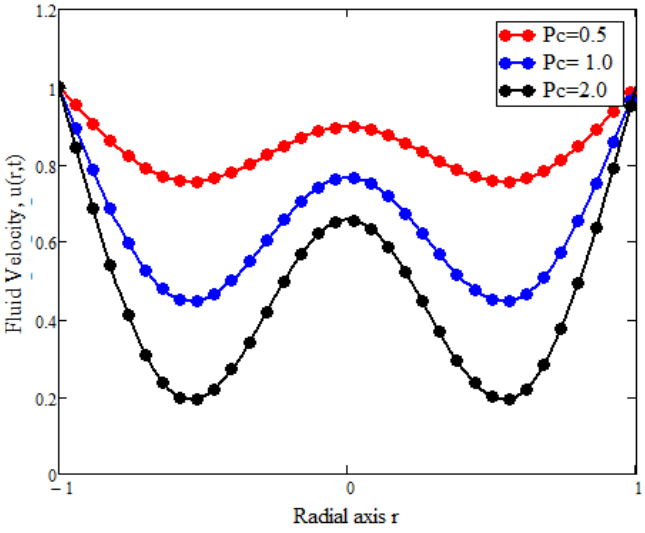

Fig.7; Particle Concentration parameter influence on fluid velocity profile at t = 5

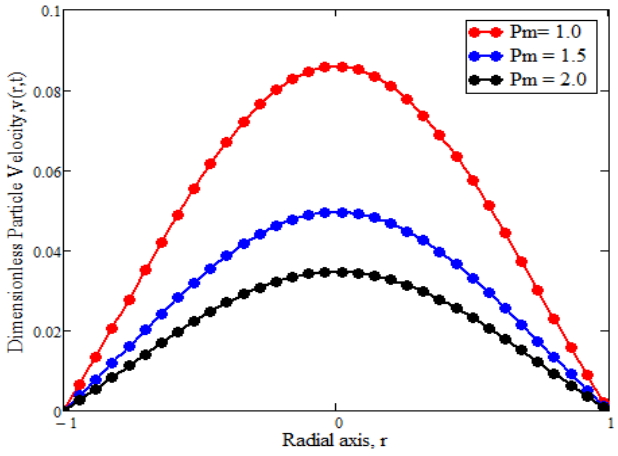

Fig.8; Particle Mass parameter influence on particle velocity profile at t = 5

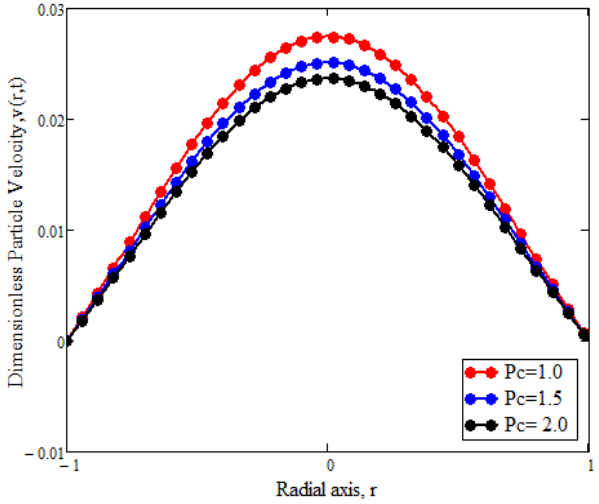

Fig.9; Particle Concentration parameter influence on particle velocity profile at t = 5

In Figure 2, the graph visually illustrates how the increase in blood temperature is directly associated with the rise in Nanoparticles volume fraction (φ). Specifically, gold Nanoparticles stand out for their exceptionally high thermal conductivity, making them efficient heat conductors. When introduced into the bloodstream, these gold Nanoparticles contribute significantly to the elevation of blood temperature, enhancing the overall heat transfer process. This temperature increase triggers a convective phenomenon, initiating a density gradient within the blood flow. Consequently, blood Nanoparticles exhibit a movement from regions of higher temperature to colder ones until temperature equilibrium is achieved. Moreover, the heightened thermal conductivity corresponds to an increased movement of blood Nanoparticles. This is a significant observation, highlighting the crucial role of thermal conductivity in influencing the behavior of Nanoparticles within the blood flow. A similar trend in velocity and temperature profiles is identified in [19], further validating the consistency of these observations. On a related note, the decrease in blood temperature is inversely correlated with the elevation of Pr, as depicted in Figure 3. The thermal diffusivity, in turn, exhibits an inverse relationship with Pr. A higher Pr value facilitates rapid heat diffusion, consequently leading to a noticeable decrease in blood temperature. This intricate interplay between thermal properties and blood temperature provides valuable insights into the dynamic behavior of blood Nanoparticles, emphasizing the significance of these factors in the context of biomedical applications and understanding thermal processes in the human body. In both scenarios of slip and no-slip conditions, the blood velocity behavior in the presence of nanoparticles shows a significant decrease as the magnetic parameter (M) increases. This trend is evident in Figures 4 and 5 at time instances t=0.6t and t=5.0, respectively. The observed reduction can be attributed to the resistive force, known as the Lorentz force, which opposes the blood flow. The Lorentz force arises from the interaction between the induced current, generated by the blood flow functioning as an electrically conducting fluid, and the magnetic field, leading to a decrease in blood flow. It is important to emphasize that the observed effects are not confined solely to robust magnetic fields found in technologies such as magnetic resonance imaging (MRI). Weaker magnetic fields within the cardiovascular system and external electronic devices like TVs and phones can also exert an influence. Shifting focus to Figures 6 and 7, these plots depict the impact of the Particle Mass Parameter and Particle Concentration Parameter on the fluid velocity profile. Changes in both parameters lead to fluid behavior closely resembling the flow of human blood through small arteries [17]. Analyzing these graphs over a broader time interval at t=5 reveals that an increase in both parameters results in an augmentation of blood nanofluid flow near the boundary. This augmentation gradually diminishes as the flow progresses towards the center of the cylinder, regardless of slip velocity conditions. This behavior is explained by a reduction in fluid yield stress near the boundary, requiring only a minimal force to initiate flow. However, as the blood nanofluid progresses towards the center, internal friction increases, leading to a subsequent reduction in flow. This comprehensive understanding sheds light on the intricate dynamics influenced by these parameters, providing valuable insights into potential applications in biomedical contexts.

Figures 8 and 9 were meticulously generated to provide a visual representation of the influence exerted by particle concentration and mass parameters on particle velocity, respectively. Upon close examination of both figures, a discernible pattern emerges, revealing that an increase in the values of these parameters leads to a notable reduction in the particle velocity profile. Upon scrutinizing the same figures, it becomes apparent that the velocity is at its peak at the center of the artery but undergoes a substantial decrease as it progresses towards the axis of flow ($-1 \leq y \leq 0.5$). In contrast, the reduction in velocity is more gradual in the region of ($0.5 \leq r \leq 1$). This insightful observation suggests that these parameters can be considered detrimental factors for blood flow, especially in the context of breast cancer treatment. The heightened values of particle concentration and mass parameters play a pivotal role in inducing a significant decrease in particle velocity. This decrease in velocity implies potential impediments to the fluid dynamics

relevant to scenarios involving breast cancer treatment. The intricate relationship between these parameters and particle velocity underscores the need for a nuanced understanding of their impact on blood flow, particularly in the context of medical interventions such as breast cancer treatment.

6. Conclusion

The overarching conclusion derived from the finding of this research work underscores the considerable potential inherent in the integration of gold nanoparticles and magnetohydrodynamic (MHD) blood flow within a comprehensive mathematical model. This integration is particularly pertinent to the realm of targeted drug delivery, specifically in the context of breast cancer therapy. The study places a significant emphasis on the pivotal role played by this innovative approach in optimizing drug delivery strategies, with a primary objective of minimizing systemic side effects while concurrently maximizing the therapeutic impact on breast cancer. The research, as outlined in the findings, serves as a valuable contribution to the scientific understanding of the intricate interplay among MHD blood flow, slip conditions, and gold nanoparticles. This interconnection is highlighted as a promising avenue with the potential to substantially enhance the precision of drug delivery. By delving into the complexities associated with breast cancer treatment, the study provides essential insights that could pave the way for more effective and targeted therapeutic interventions. In essence, the general conclusion from the file underscores the transformative potential of this integrated approach, positioning it as a promising frontier in the ongoing pursuit of refining drug delivery methods for the treatment of breast cancer. The multifaceted considerations encompassing MHD blood flow, slip conditions, and gold nanoparticles collectively contribute to the development of a holistic and sophisticated model, poised to address the challenges inherent in current breast cancer treatment strategies.

Availability of Data and Materials:
Not applicable

Conflict of Interest:
The authors declare that there are no conflicts of interest related to the study. This is an important declaration to ensure transparency and to address any potential biases that could arise from financial or personal relationships.

Funding:
The study was supported by the Tertiary Education Trust Fund (TETFund).

Authors' Contributions Statement:
The statement indicates that all authors contributed equally to the work and approved the final version of the manuscript.

Acknowledgment:
The work is acknowledged as being supported by TETFund. This is a formal acknowledgment of the financial support received for the research.

References

[1] A. Brown and B. White, "Understanding Slip Conditions in Small Arteries," Journal of Cardiovascular Modeling, vol. **10**, no. **3**, pp. **45-56, 2019**.

[2] X. Chen, "Integration of Gold Nanoparticles in Blood Flow Modeling: Implications for Breast Cancer Treatment," Journal of Nanomedicine, vol. **15**, no. **2**, pp.**78-91, 2021**.

[3] J. Doe, "Gold Nanoparticles as Drug Delivery Vehicles in Cancer Therapy," Journal of Drug Delivery, vol.**8**, no.**4**, pp. **112-125, 2019.**

[4] J. Doe, "Personalized Treatment Strategies: A Mathematical Modeling Approach," Cancer Research, vol. **25**, no. **3**, pp. **210-225, 2021.**

[5] R.JonesandL.Smith,Magnetohydrodynamics in Blood Flow Modeling: Current Insights," Physics in Medicine and Biology, vol. **12**, no. **1**, pp. **34-47, 2017**.

[6] M. Johnson, "Comprehensive Mathematical Model for Breast Cancer Treatment Optimization, "Journal of Mathematical Medicine, vol. **18**, no. **4**, pp. **189-201, 2023**.

[7] Y. Kim and S. Lee, "Gold Nanoparticles as Targeted Drug Delivery Vehicles: A Review," Journal of Nanoscience and Nanotechnology, vol. **20**, no. **6**, pp. **3567-3583, 2018.**

[8] H. Patel, "The Influence of Magnetohydrodynamics on Drug Transport in the Bloodstream," Journal of Applied Physiology, vol. **15**, no. **7**, pp. **234-245, 2022**.

[9] S. Maiti, S. Shaw, and G. C. Shit, "Fractional order model for thermochemical flow of blood with Dufour and Soret effects under magnetic and vibration environment," Colloids Surfaces B Biointerfaces, vol. **197**, **111395, 2021**.

[10] J. Raza, "Thermal radiation and slip effects onmagnetohydrodynamic(MHD) stagnation point flow of Casson fluid over aconvective stretching sheet," Propuls. Power Res., vol. **18**, pp. **138-146, 2019**.

[11] K. Benhanifia et al., "Investigation of mixing viscoplastic fluid with a modified anchor impeller inside a cylindrical stirred vessel using Casson–Papanastasiou model," Sci. Rep., vol. **12**, pp. **1–19, 2022**.

[12] A. Imtiaz et al., "Generalized model of blood flow in a vertical tube with suspension of gold nanomaterials: Applications in cancer therapy," Comput. Mater. Contin., vol. **65**, pp. **171–192, 2020.**

[13] W. N. N. NoranuarMohamad et al.,"Non-coaxial rotation flow of MHD Casson nanofluid carbon nanotubes past a moving disk with porosity effect," Ain Shams Eng. Journal, vol. **12**, pp. **4099-4110, 2021**.

[14] J. Mackolil and B. Mahanthesh, "Exact and statistical computations of radiated flow of nano and Casson fluids under heat and mass flux conditions," J. Comput. Des. Eng., vol. **6**, pp. **593–605, 2019**.

[15] H. F. Oztop and E. Abu-Nada, "Numerical study of natural convection in partially heated rectangular enclosures filled with nanofluids," Int. J. Heat Fluid Flow, vol. **29**, pp. **1326–1336, 2008.**

[16] R.Padma, R. Selvi, and R. T. Ponalagusamy, "Effects of slip and magnetic field on the pulsatile flow of a Jeffrey fluid with magnetic nanoparticles in a stenosed artery," Eur. Phys. J. Plus, vol. **134**, pp. **1–15, 2019.**

[17] I. Khan et al., "Natural convection heat transfer in an oscillating vertical cylinder," PLoS One, vol. 13, pp. e0188656, 2018.

[18] I. A. Mirza et al., "Flows of a generalized second grade fluid in a cylinder due to a velocity shock," Chinese J. Phys., vol. **60**, pp. **720–730, 2019**.

[19] S. Maiti, S. Shaw, and G. C. Shit, "Caputo–Fabrizio fractional order model on MHD blood flow with heat and mass transfer through a porous vessel in the presence of thermal radiation," Phys. A Stat. Mech. its Appl., vol. **540, 123149, 2020.**

[20] M. H. Esfe et al., "A critical review on pulsating flow in conventional fluids and nano fluids:Thermo-hydraulic characteristics," Int. Commun. Heat Mass Transf., vol. **120, 104859, 2021**.

